

# Corrosion behaviour in acidic environments of alloy 625 produced by Material Extrusion: effect of the process-generated microstructure and defects

T. Persico, S. Lorenzi, M. Cabrini, L. Nani, T. Pastore, G. Barbieri, F. Cognini

Additive manufacturing (AM) is gaining increasing interest in various strategic industrial sectors such as Oil & Gas, aerospace, and chemical industries. This group of technologies includes both innovative yet well-established techniques and more recent methods like Material Extrusion (MEX). This technique shows several advantages over other AM techniques, including high deposition rates and simplicity in feedstock material handling; however, it presents numerous endogenous macro-defects that can affect the corrosion resistance. The relationship between the defects of this technology and its corrosion behaviour still needs to be thoroughly investigated. This work studies the relationship between microstructure, internal defects, and corrosion behaviour in reducing acidic environments of alloy 625 obtained through MEX, compared to the same alloy obtained with traditional technology. The results lay the groundwork for further studies aimed to study the relationship between microstructure and corrosion behaviour of alloy 625 obtained with other AM technologies.

**KEYWORDS:** ADDITIVE MANUFACTURING, CORROSION, NICKEL SUPERALLOY, MICROSTRUCTURE, DEFECTS

## INTRODUCTION

Alloy 625 (UNS N06625) is a highly alloyed nickel-base alloy that presents good mechanical strength, high corrosion resistance in several environments, creep resistance and weldability. Because of this attractive combination of properties, alloy 625 has found widespread applications in sectors such as nuclear, Oil&Gas, energy, chemical and aerospace [1], [2], [3]. The high levels of Cr, Mo and Nb provide good corrosion resistance, especially for localized corrosion, increasing the pitting resistance equivalent number (PREN) [4]. Furthermore, Nb reduces the deleterious effect of Mo and Cr precipitates at the grain boundary on the resistance to intergranular corrosion [5]. The Al and Ti additions are primarily for refining purposes, while Fe provides further solid solution strengthening [3]. Alloy 625 is typically used for the production of fluid-dynamic parts and valves components for the energy and Oil&Gas sectors and is commonly manufactured by plastic deformation processes and subsequent machining. Concerning the machinability, alloy 625 usually leads to excessive tool wear and high material removal rates. Consequently, the

**T. Persico, S. Lorenzi, M. Cabrini,  
L. Nani, T. Pastore**

Department of Engineering and Applied Sciences,  
Università degli studi di Bergamo, Italy

**G. Barbieri, F. Cognini**

Department for Sustainability - Research Centre of Casaccia,  
ENEA, Rome, Italy

cost of the manufactured part can significantly increase with the complexity of the final geometry. [6], [7].

Additive Manufacturing (AM) technologies can be successful for nickel alloys because they achieve high material utilization efficiencies, do not cause tool wear and can manufacture complex geometries without a substantial increase of the cost [8], [9]. Additive manufacturing is a family of technologies that deposits materials layer by layer to create geometric 3D components. The most common technologies utilize metal powder or wire as feedstock. These techniques melt the metallic material in the printing process, so the product is ready for the usage [1], [10]. The high cooling speed provides completely different microstructures with respect to the traditional worked alloys, generally with higher mechanical properties. Despite, the main disadvantages of AM technologies are speed and production costs. To overcome these difficulties, new techniques have been developed to require a much simpler and cheaper printing equipment with much higher production speeds [11]. This is achieved by using an auxiliary polymer as in material extrusion (MEX) technology. The printing process involves the deposition of a polymer filament filled with metal powders. Conversely, traditional additive technologies, there is not the melting of the metal powder during the deposition. Post-deposition treatments are mandatory: debinding to remove the polymer and sintering to consolidate the metal powders [12], [13]. Previous studies have shown that MEX technology

presents elongated and interconnected macro-defects with periodic distribution within the material, depending on the adopted deposition strategy [13]. The aim of this work is to investigate the relationship between corrosion behaviour, microstructure and defects of an alloy 625 obtained by MEX and to compare it with the results obtained by the same alloy produced by hot working (HW) by means of corrosion tests in sulfuric acid at different temperatures.

## MATERIALS AND METHODS

### Materials

MEX-processed specimens were made with a MetalXMarkforged System using commercial alloy 625 powder-filled polymer filament of approximately 1.8 mm in diameter as feedstock material. Following the sintering process, the material has a composition reported in Tab. 1. The specimens consist of 5 mm x Ø 15 mm cylinders composed of two zones with different scanning strategies. The outer area, named contour, is filled with 4 stripe-thick with parallel direction between successive layers. The core, defined as the inner zone, is realized with layers with deposition directions alternately oriented at +45° and -45°. The HW material consisted in hot-rolled bar with a diameter of 16 mm (chemical composition reported in Table 1) that was heat treated and then mechanically cut to get 5 mm thick specimens. The performed heat treatment is a "Grade 1" following ASTM B446: solubilization at 980 °C for 32 minutes and quenching in water.

**Tab. 1** - Composizioni chimiche della lega 625 prodotta tramite MEX e HW / Chemical compositions of alloy 625 produced by MEX and HW

| Technology | Element (% weight) |      |      |       |       |       |      |      |       |       |        |       |      |      |
|------------|--------------------|------|------|-------|-------|-------|------|------|-------|-------|--------|-------|------|------|
|            | C                  | Si   | Mn   | P     | S     | Cr    | Mo   | Ni   | Nb    | Ti    | Al     | Co    | Ta   | Fe   |
| MEX        | 0,08               | 0,52 | 0,40 | 0,006 | 0,004 | 19,55 | 8,57 | Bal. | 3,28  | 0,022 | <0,001 | 0,047 | -    | 2,61 |
| HW         | 0,036              | 0,25 | 0,19 | 0,007 | 0,001 | 21,60 | 8,26 | Bal. | 3,660 | 0,243 | 0,199  | 0,02  | 0,01 | 3,11 |

### Microstructural investigation and defects characterization

The specimens were analyzed after grinding with silicon carbide emery papers up to 4000 grit and subsequently polishing with 1 µm diamond suspension. The specimens have been investigated with a digital-optical microscope

(OM) Keyence VHX-7100 and a field emission scanning electron microscope (FESEM) Zeiss Sigma 300 equipped with an Oxford x-Act probe for energy dispersive X-ray spectroscopy (EDS). For metallographic analysis, the etching solution 15-10-10 (HCl, HNO<sub>3</sub>, CH<sub>3</sub>COOH) was used.

### Corrosion immersion test in sulfuric acid

Immersion corrosion tests were carried out according to ASTM G31 in a 50% (wt.%)  $H_2SO_4$  solution at 50°C, 80°C and boiling temperature. The specimens were placed in a 1 L Erlenmeyer flask with a reflux condenser to avoid the evaporation of the test solution. At the bottom of the flask, a thin layer of boiling chips was spread in order to promote the boiling and avoid the contact between the specimens and the flask background. The cell was heated by a thermostatic bath and the test solution temperature was monitored by internal thermometer. Before the tests, all the specimens underwent mechanically grinding using SiC emery papers up to 4000 grit and then polishing with 1  $\mu m$  diamond suspension. Then, they were weighted 3 times before the immersion. After 24 hours of immersion,

the specimens were extracted from the solution, washed with distilled water and rinsed in acetone, then weighted again to establish the weight loss. All the corroded specimens were further analysed (OM/SEM/EDS).

### RESULTS AND DISCUSSION

Microstructural investigation and defects characterization The MEX-fabricated specimens showed a microstructure with equiaxed austenitic grains and several precipitates, as visible in Figure 1A. Moreover, typical macro-defects of MEX technology were also visible under digital optical microscope. Hot worked specimens were characterized as well by austenitic equiaxed grains with characteristic twins as shown in Fig. 1B, with finer grains with respect to MEX specimens.

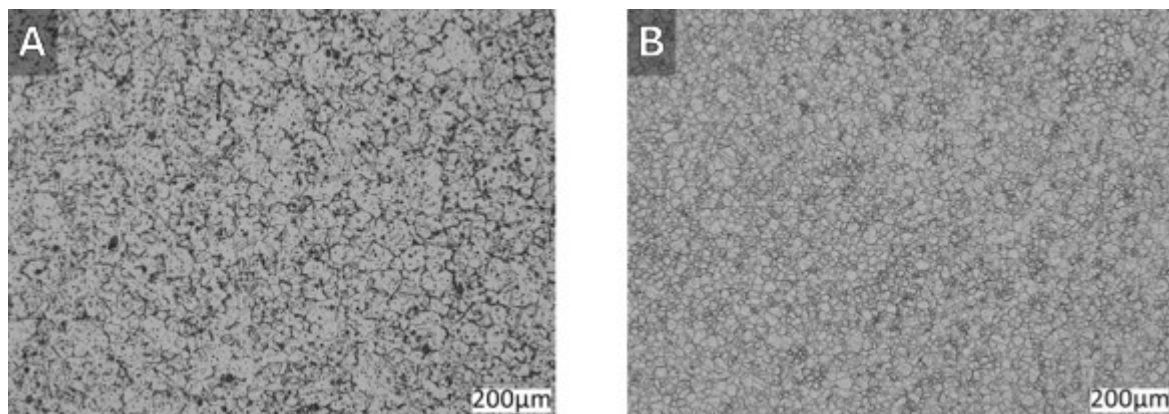


**Fig.1** - Metallografia x200 della lega 625 ottenuta per MEX A) e HW B). / Metallography of alloy 625 processed by MEX A) and HW B).

EDS analysis detected carbides of Ni e Mo in alloy 625 manufactured via MEX, as shown in Fig. 2A. It is focal to specify that such carbides are homogeneously arranged and in block shapes in the core, while they are elongated and primarily arranged along the grain boundaries in the contour. Furthermore, inclusions of oxides rich in Al, Si, and Cr and surrounded by a secondary phase were discovered (Fig. 2B). In literature, it has been proposed that oxides and carbides form during debinding and

sintering by the capture of impurities [14], [15]. The reference HW material is characterised by the presence of carbides, both in blocks and elongated along the grain boundary forming semi-continuous chains, as visible in Fig. C. Second phases rich of titanium were also detected in HW specimens.

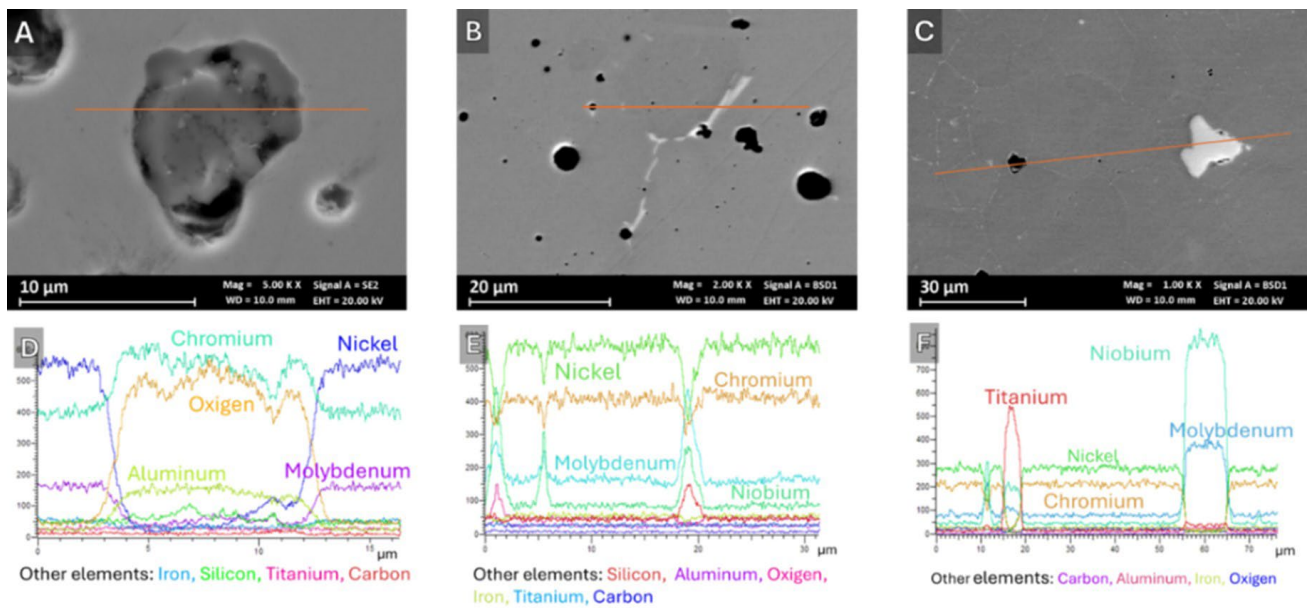


**Fig.2** - Analisi EDS di provini MEX A), B), D), E) e HW C), F) / EDS Analysis of MEX A), B), D), E) and HW C), F)

### Corrosion tests in sulfuric acid

The weight losses in 50% sulfuric acid solution showed an exponential trend depending on the temperature of the solution, as seen in Fig. 3. At higher temperatures, there

is an increase of the movement of ions and reduction of oxygen concentration all contributing to higher corrosion rates [16], [17].

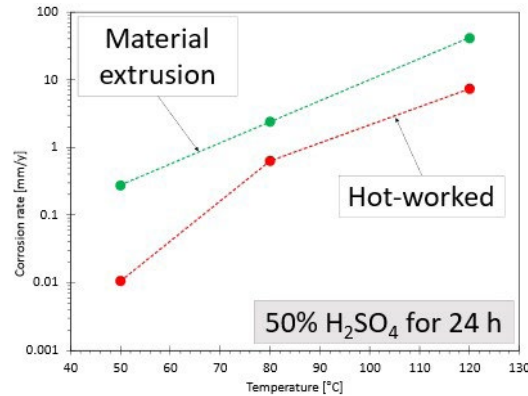


**Fig.3** - Velocità di corrosione della lega 625 in 50% H<sub>2</sub>SO<sub>4</sub> in funzione della temperatura della soluzione / Corrosion rates vs solution temperature of alloy 625 in 50% H<sub>2</sub>SO<sub>4</sub>

The corrosion rate of alloy 625 HW is comparable with the values already reported in the literature [18], [19]. Conversely, MEX exhibited corrosion rates an order of magnitude higher than those of the alloy obtained through traditional technology. Furthermore, MEX showed high corrosion rates already at 50 °C, while HW displayed significantly lower corrosion rates at that temperature. Digital optical microscope analysis of the exposed surfaces proved that the corrosion attacks morphology

in both MEX and HW preferentially follows the grain boundaries, as shown in Fig. 4.

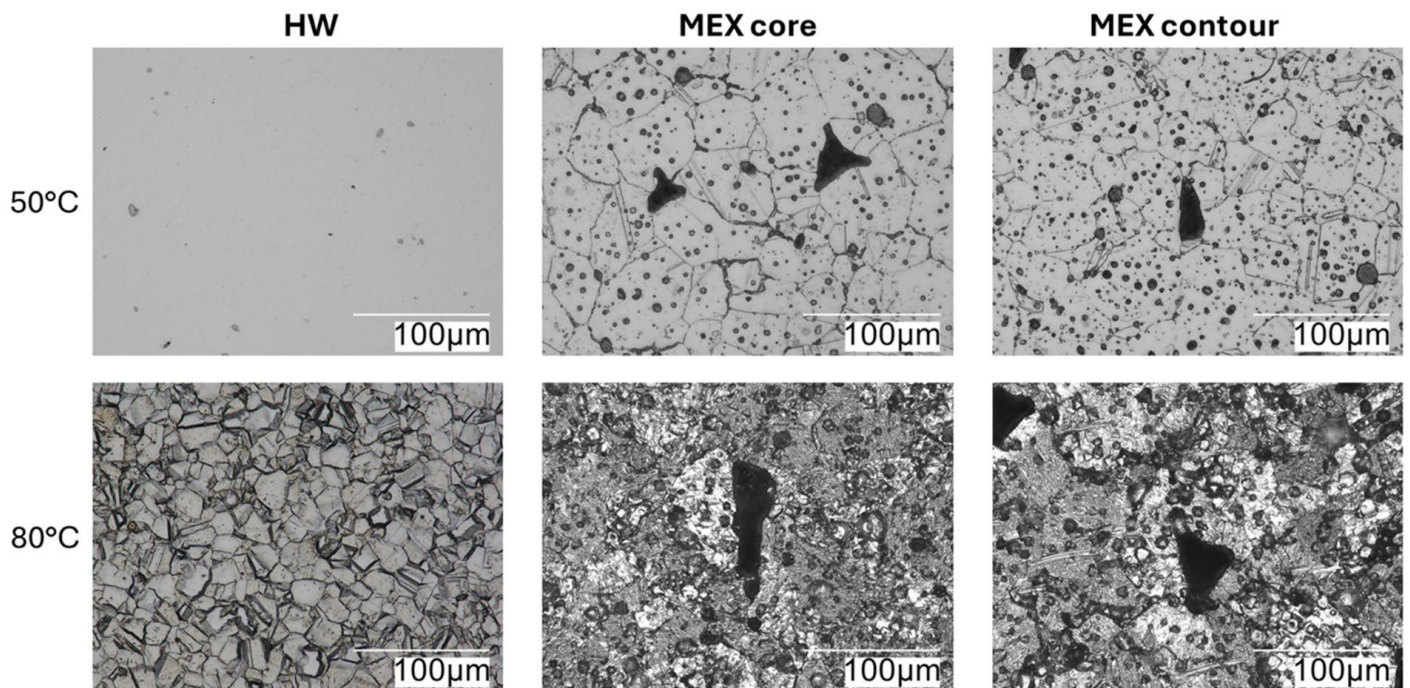


**Fig. 4** - Superfici della lega 625 dopo le prove di immersione in  $H_2SO_4$  a 50°C e 80°C – Surface of alloy 625 after immersion test in  $H_2SO_4$  at 50°C and 80°C.

EDS of alloy 625 after the immersion test demonstrated that the interface between carbides/Ni-grain and oxides/Ni-grain is the predominant site where the corrosion occurs (Fig. 5). Therefore, it is plausible that the intergranular corrosion behaviour of Alloy 625 in both HW

and MEX is highly affected by the presence of carbides with adjacent Ni and Cr depleted zones, distributed along the grain boundaries [20].

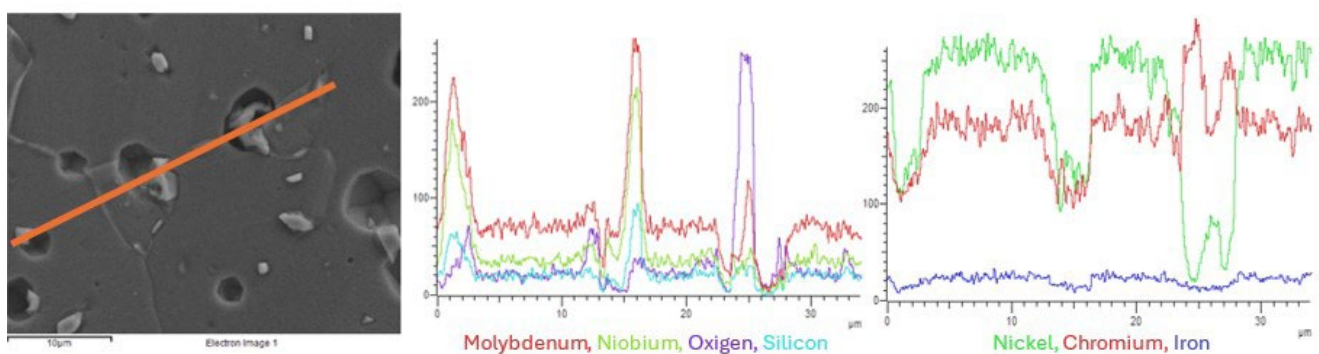


**Fig. 5** - Analisi EDS di un provino MEX a seguito della prova di immersione in  $H_2SO_4$  a 50°C - EDS Analysis of MEX specimen after immersion test in  $H_2SO_4$  at 50°C.

During immersion test, macro-defects of alloy 625 MEX increased in size because of severe corrosion occurring. The defect size increased greatly with the aggressiveness of the solution, as visible in Fig. 6. The enlargement of defects leads to an expansion of surface exposed to

the corrosive environment, contributing to the higher corrosion rates observed in MEX specimens if compared to the HW benchmark.

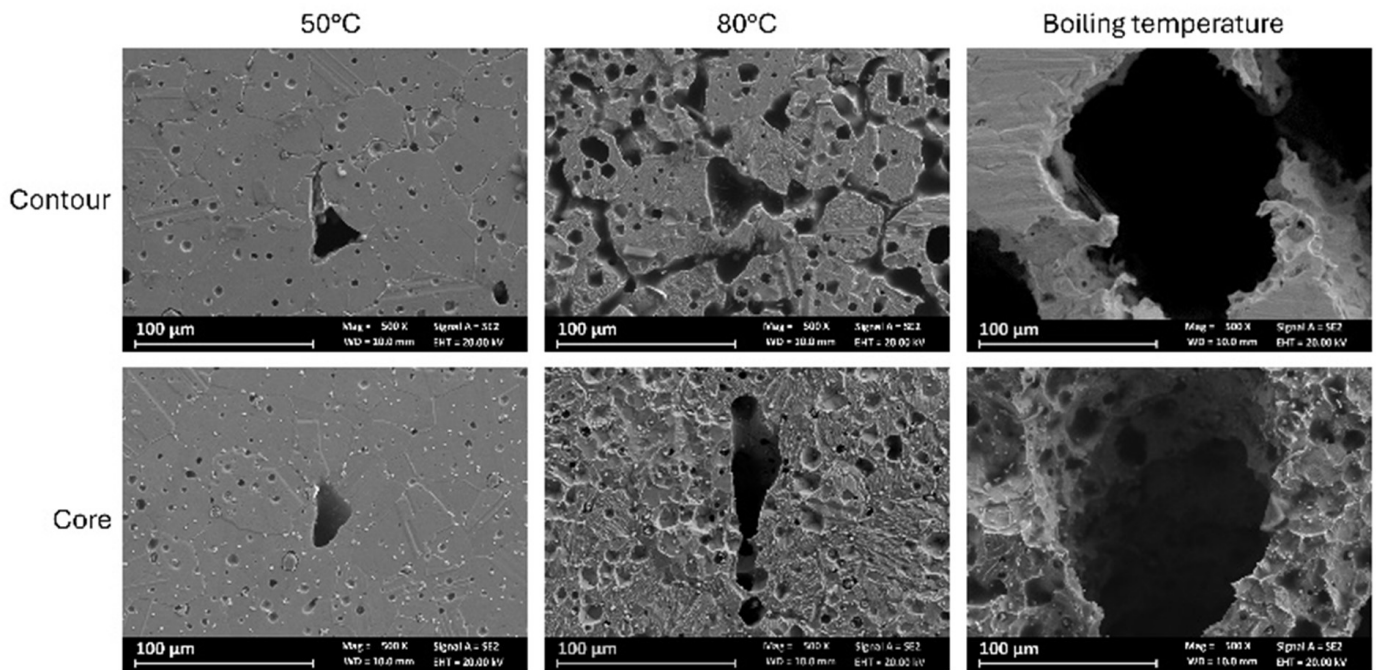


**Fig. 6** - Macro-difetti dei provini MEX post immersione in H<sub>2</sub>SO<sub>4</sub> a differenti temperature / MEX macro-defects after immersion test in H<sub>2</sub>SO<sub>4</sub> at different temperature.

At all test temperatures, there was a distinct difference of corrosion morphology between core and contour in the MEX samples. In both regions, it is evident that the corrosive attack initiates at the interface between the carbides and the base material. In the contour, the corrosion is strictly intergranular, while the core showed a more homogeneous morphology. This observation is consistent with the different carbide arrangements and shapes in the core and contour.

## CONCLUSIONS

This study investigated the alloy 625 produced via Material Extrusion in terms of internal defects, microstructure and corrosion behaviour. The research aimed to understand how the material obtained through MEX may exhibit different corrosion behaviour compared to the same material produced traditionally. This work lays the foundation to characterize the corrosion behaviour of further additive manufacturing technologies. The main highlighted findings are as follows:

- Both technologies provide austenitic equiaxed grains. MEX specimens showed homogeneously distributed carbides with block shapes within the

core, while in the contour they were elongated and primarily aligned along grain boundaries. HW material is also characterised by carbides, both in blocks and elongated along the grain edge forming semi-continuous chains.

- Corrosion immersion tests in sulfuric acid demonstrated that Alloy 625 produced by MEX exhibited corrosion rates significantly higher than those produced by HW. Intergranular corrosion mechanism occurs in both HW and MEX specimens, predominantly in the contour region.
- During the corrosion test, the macro-defects widened significantly. This indicates that in areas where the material exhibits active behaviour, the macro-defects characteristic of MEX technology have a deleterious effect.

## ACKNOWLEDGEMENTS

This research was funded by the European Union, NextGenerationEU program: MICS – Made in Italy circolare e sostenibile, spoke 6.04 Development of new alloys with improved properties and decreased environmental impact for AM powder production.

## BIBLIOGRAFIA

- [1] M. Karmuhilan and S. Kumanan, "A Review on Additive Manufacturing Processes of Inconel 625," *J Mater Eng Perform*, vol. 31, no. 4, pp. 2583–2592, Apr. 2022, doi: 10.1007/S11665-021-06427-3/TABLES/5.
- [2] V. Shankar, K. Bhanu Sankara Rao, and S. L. Mannan, "Microstructure and mechanical properties of Inconel 625 superalloy," *Journal of Nuclear Materials*, vol. 288, no. 2–3, pp. 222–232, Feb. 2001, doi: 10.1016/S0022-3115(00)00723-6.
- [3] S. Floreen, G. E. Fuchs, and W. J. Yang, "The Metallurgy of Alloy 625," *Superalloys 718, 625, 706 and Various Derivatives (1994)*, pp. 13–37, Aug. 1994, doi: 10.7449/1994/SUPERALLOYS\_1994\_13\_37.
- [4] E. L. Hibner, "CORROSION/86," *NACE International*, vol. paper no. 181, 1986.
- [5] G. D. E. N. C. Smith, "The effect of niobium on the corrosion resistance of nickel-base alloys," *Proc Int Symp Niobium High Temp Appl*, 2004.
- [6] Y. L. Hu, X. Lin, X. B. Yu, J. J. Xu, M. Lei, and W. D. Huang, "Effect of Ti addition on cracking and microhardness of Inconel 625 during the laser solid forming processing," *J Alloys Compd*, vol. 711, pp. 267–277, Jul. 2017, doi: 10.1016/J.JALLCOM.2017.03.355.
- [7] Y. AbouelNour and N. Gupta, "In-situ monitoring of sub-surface and internal defects in additive manufacturing: A review," *Mater Des*, vol. 222, Oct. 2022, doi: 10.1016/J.MATDES.2022.111063.
- [8] G. Sander et al., "Corrosion of Additively Manufactured Alloys: A Review," *Corrosion*, vol. 74, no. 12, pp. 1318–1350, Dec. 2018, doi: 10.5006/2926.
- [9] W. E. Frazier, "Metal additive manufacturing: A review," *J Mater Eng Perform*, vol. 23, no. 6, pp. 1917–1928, Apr. 2014, doi: 10.1007/S11665-014-0958-Z/FIGURES/9.
- [10] M. Cabrini et al., "Stress corrosion cracking of additively manufactured alloy 625," *Materials*, vol. 14, no. 20, p. 6115, Oct. 2021, doi: 10.3390/MA14206115/S1.
- [11] J. M. Costa, E. W. Sequeiros, M. T. Vieira, and M. F. Vieira, "Additive Manufacturing: Material Extrusion of Metallic Parts," *U.Porto Journal of Engineering*, vol. 7, no. 3, pp. 53–69, Apr. 2021, doi: 10.24840/2183-6493\_007.003\_0005.
- [12] Y. Thompson, J. Gonzalez-Gutierrez, C. Kukla, and P. Felfel, "Fused filament fabrication, debinding and sintering as a low cost additive manufacturing method of 316L stainless steel," *Addit Manuf*, vol. 30, p. 100861, Dec. 2019, doi: 10.1016/J.ADDMA.2019.100861.
- [13] A. Carrozza et al., "A comparative analysis between material extrusion and other additive manufacturing techniques: Defects, microstructure and corrosion behavior in nickel alloy 625," *Mater Des*, vol. 225, p. 111545, Jan. 2023, doi: 10.1016/J.MATDES.2022.111545.
- [14] K. Horke, A. Meyer, and R. F. Singer, "Metal injection molding (MIM) of nickel-base superalloys," *Handbook of Metal Injection Molding*, pp. 575–608, Jan. 2019, doi: 10.1016/B978-0-08-102152-1.00028-3.
- [15] Y. Thompson et al., "Metal fused filament fabrication of the nickel-base superalloy IN 718," *J Mater Sci*, vol. 57, no. 21, pp. 9541–9555, Jun. 2022, doi: 10.1007/S10853-022-06937-Y/FIGURES/8.
- [16] A. Mishra, "Performance of corrosion-resistant alloys in concentrated acids," *Acta Metallurgica Sinica (English Letters)*, vol. 30, no. 4, pp. 306–318, Apr. 2017, doi: 10.1007/S40195-017-0538-Y/TABLES/3.
- [17] P. Pedferri, "Uniform Corrosion in Acidic and Aerated Solutions," *Engineering Materials*, pp. 145–167, 2018, doi: 10.1007/978-3-319-97625-9\_8.
- [18] ASM, "ASM Handbook Volume 13: Corrosion," *ASM Metals Handbook*, pp. 1–1135, 2003, Accessed: Jul. 20, 2023.
- [19] "HAYNES® 625 alloy - Haynes International." Accessed: Jul. 16, 2024. [Online]. Available: <https://haynesintl.com/en/datasheet/haynes-625-alloy/#iso-corrosion-diagrams>
- [20] A. K. Jena and M. C. Chaturvedi, "The role of alloying elements in the design of nickel-base superalloys," *J Mater Sci*, vol. 19, no. 10, pp. 3121–3139, Oct. 1984, doi: 10.1007/BF00549796/METRICS.

# Comportamento a corrosione in ambienti acidi della lega 625 prodotta mediante Material Extrusion: effetto della microstruttura e delle porosità generate dal processo produttivo

La manifattura additiva (AM) sta acquistando sempre maggiore interesse in diversi settori industriali come quelli dell'Oil&Gas, aerospaziale e chimico. Questo gruppo di tecnologie comprende tecniche innovative ma ben consolidate, nonché metodi più recenti come la Material Extrusion (MEX). Questa tecnica mostra vantaggi rispetto alle altre tecniche AM, tra cui l'elevata velocità di deposizione e la semplicità nella gestione della materia prima; tuttavia, presenta numerose macro-porosità endogene che possono influenzare la resistenza alla corrosione. La relazione fra i difetti di questa tecnologia e il suo comportamento a corrosione è ancora da approfondire. Questo lavoro studia la relazione fra la microstruttura, i difetti interni e il comportamento a corrosione in ambiente acido riducente della lega 625 ottenuta tramite MEX, rispetto alla lega ottenuta con tecnologia tradizionale. I risultati pongono le basi per ulteriori approfondimenti volti allo studio della relazione fra microstruttura e comportamento a corrosione della lega 625 prodotta mediante altre tecnologie AM.

**PAROLE CHIAVE:** MANIFATTURA ADDITIVA, CORROSIONE, SUPERLEGHE DI NICKEL, MICROSTRUTTURA, DIFETTI

[TORNA ALL'INDICE >](#)